

VDInstruct: Zero-Shot Key Information Extraction via Content-Aware Vision Tokenization

Son Nguyen[†], Giang Nguyen[♦], Hung Dao[†], Thao Do[†], Daeyoung Kim[†]
KAIST, South Korea[†], Auburn University, US[♦]

{nguyendinhson, hiechehe, thaodo, kimd}@kaist.ac.kr[†], nguyengiangbkhn@gmail.com[♦]

Abstract

Key Information Extraction (KIE) underpins the understanding of visual documents (e.g., receipts and contracts) by extracting precise semantic content and accurately capturing spatial structure. Yet existing multimodal large language models (MLLMs) often perform poorly on dense documents and rely on vision tokenization approaches that scale with image size, leading to redundant computation and memory inefficiency. To address these challenges, we introduce VDINSTRUCT, an MLLM that separates spatial region detection from semantic feature extraction. Central to our model is a content-aware tokenization strategy: rather than fragmenting the entire image uniformly, it generates tokens in proportion to document complexity, preserving critical structure while eliminating wasted tokens. Leveraging a three-stage training paradigm, our model achieves state-of-the-art (SOTA) results on KIE benchmarks, matching or exceeding the accuracy of leading approaches while reducing the number of image tokens by roughly $3.6\times$. In zero-shot evaluations, VDINSTRUCT surpasses strong baselines—such as DocOwl 1.5—by $+5.5$ F1 points, highlighting its robustness to unseen documents. These findings show that content-aware tokenization combined with explicit layout modeling offers a promising direction forward for document understanding. Data, source code, and model weights will be made publicly available.

1. Introduction

Visual Document Understanding (VDU) refers to the automated processing of documents (e.g., invoices, receipts, or contracts) that contain both rich visual and textual content. VDU involves extracting text and pinpointing its exact location on the page, identifying structural components like headings, columns, and charts, and interpreting how these elements interact to convey overall information. Within this framework, Key Information Extraction (KIE) serves as the core task: it focuses on locating and extracting the most

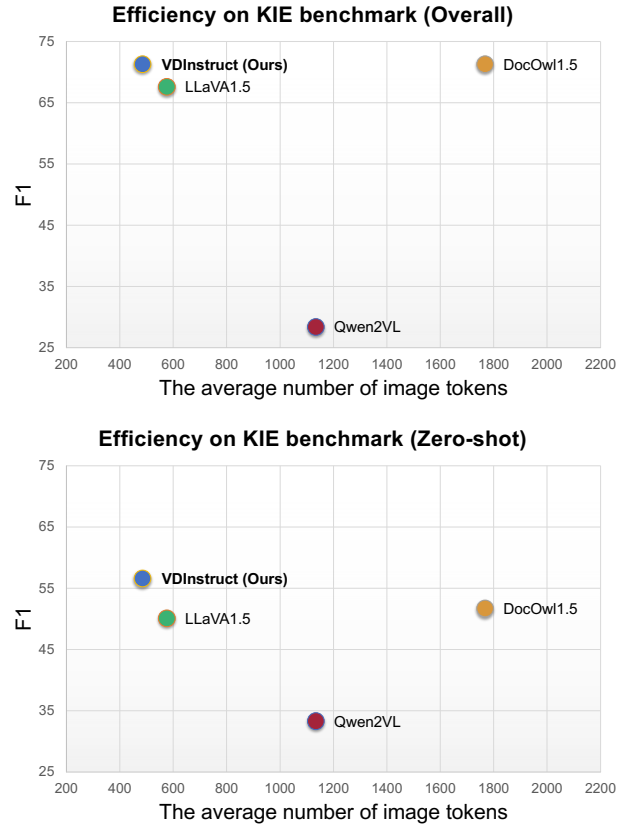


Figure 1. Image-token consumption (efficiency) and F1 scores on overall and out-of-domain (zero-shot) KIE benchmarks. VDINSTRUCT achieves SOTA F1 scores while using ≈ 500 image tokens per page— $3.6\times$ fewer than DocOwl 1.5 [13].

critical fields—such as vendor names, dates, item descriptions, amounts, or contractual clauses—from diverse document types, thereby enabling a wide range of downstream applications [48].

However, while existing foundation models for VDU like LayoutLM [51], Donut [19], and DocFormer [1] achieve strong results by fusing text, visual cues, and spa-

tial layout, this performance comes at the cost of extensive domain-specific data annotation and expensive supervised fine-tuning. Each new document type requires collecting labeled examples and often fine-tuning a separate model. In addition, they often struggle to generalize to new document formats without additional annotations, driving the need for more scalable and robust methods that can adapt to diverse layouts and content with minimal supervision.

Multimodal large language models (MLLMs), for example, the LLaVA family [27], have shown remarkable zero-shot performance on natural-image visual question answering (VQA) via large-scale vision language pretraining combined with instruction tuning. Yet, when applied to VDU, MLLMs often fall short, achieving low accuracy on tasks like document information localization and extraction (see Tab. 1). Unlike natural scenes, documents pack dense, fine-grained text into precise spatial layouts. Capturing these requires high-resolution inputs to preserve small tokens and subtle structural cues. However, most MLLMs downsample document images (*e.g.*, 336×336 for LLaVA 1.5) heavily to fit their context windows, sacrificing critical semantic and spatial information. To mitigate resolution loss, recent MLLMs, such as DocOwl 1.5 [13] and Qwen2VL [50], scale image-token counts with pixel resolution by adopting an adaptive cropping module. This strategy often splits a single image into multiple patches, encodes each patch separately, and then aggregates all image tokens. Although this improves accuracy, it is prone to **token explosion**, which inflates memory usage and risks context-window overflow. Moreover, naively scaling the number of image tokens with the image size results in **token redundancy**, since a high-resolution page may contain only several words, and most patches are the background.

To address these limitations, we introduce VDI_NSTRUCT, a new multimodal large language model designed for KIE with token-efficient, layout-aware visual encoding. Our work introduces two key innovations:

- **Dual Vision Encoder:** We disentangle spatial and semantic processing into two sub-encoders: a **Spatial Encoder** that is trained with our new layout-aware pre-training objective to model document structure explicitly; a **Semantic Encoder** extracts fine-grained multimodal (textual + visual) features from high-resolution inputs.
- **Rigorous Benchmark for KIE:** We curate the first comprehensive, instruction-based KIE benchmark by unifying eight diverse public document datasets—six for in-domain tuning and two held out for zero-shot robustness testing.

Through extensive experiments, we found that: firstly, VDI_NSTRUCT is more computationally efficient than state-of-the-art models since it generates only ≈ 500 tokens per page, $3.6\times$ fewer than DocOwl 1.5 (see Fig. 1). Secondly, despite significantly reducing the number of image tokens,

VDI_NSTRUCT achieves a SOTA overall performance on KIE benchmarks and sets a new record in zero-shot settings, $+5.5$ points gain of F1 scores, compared to DocOwl 1.5 [13], the previous state-of-the-art model in VDU (see Tab. 1).

2. Related Works

2.1. Multimodal LLMs for Document Understanding

Multimodal Large Language Models (MLLMs) pursue a single, task-agnostic model for document understanding, yet they diverge sharply in balancing vision input and computational cost. At one extreme, DocLLM [48] removes images altogether, supplying the LLM only with OCR tokens and their bounding boxes; its disentangled spatial attention delivers highly efficient reasoning but sacrifices non-textual cues. In contrast, mPLUG-DocOwl [53] couples a vision encoder with an instruction-tuned decoder to achieve fully OCR-free parsing, and version 1.5 [13] reduces image tokens via horizontal patch merging while preserving SOTA accuracy. Bridging these philosophies, InstructDoc shows that a single instruction-tuned VL model can zero-shot across 30 public datasets [47], while generalist systems such as Qwen-VL rival much larger models on DocVQA [34] and TextVQA [45] without document-specific tuning [2]. Despite this progress, current MLLMs [7, 11, 53, 54] either explode visual tokens at high resolution or blur fine-grained layout by aggressive down-sampling. Our dual-encoder architecture resolves this tension: a spatial branch distills layout cues and a semantic branch preserves small text and subtle graphics, together producing $3.6\times$ fewer tokens than DocOwl 1.5 yet retaining the detail essential for accurate KIE.

2.2. Key Information Extraction

Key Information Extraction (KIE) seeks to automatically surface critical fields from visually rich documents. A recent survey by Rombach and Fettke [43] highlights both the commercial impact of KIE systems and the rapid research progress driving that impact. The modern line of work began with LayoutLM [51], which first fused token embeddings with their 2-D coordinates; this simple yet powerful idea lifted F1 scores on forms and receipts far beyond those of text-only baselines. LayoutLMv2 [52] broadened the signal by injecting image patches and relative 2-D positional biases, yielding robustness to scale and rotation changes, while LayoutLMv3 [15], StrucTexTv2 [56], and SelfDoc [22] unified masked pre-training over text and pixels to push accuracy even further across multiple KIE benchmarks. Complementing this family, DocFormer [1] used cross-modal attention to explicitly align words with co-located visual features, achieving competitive accuracy

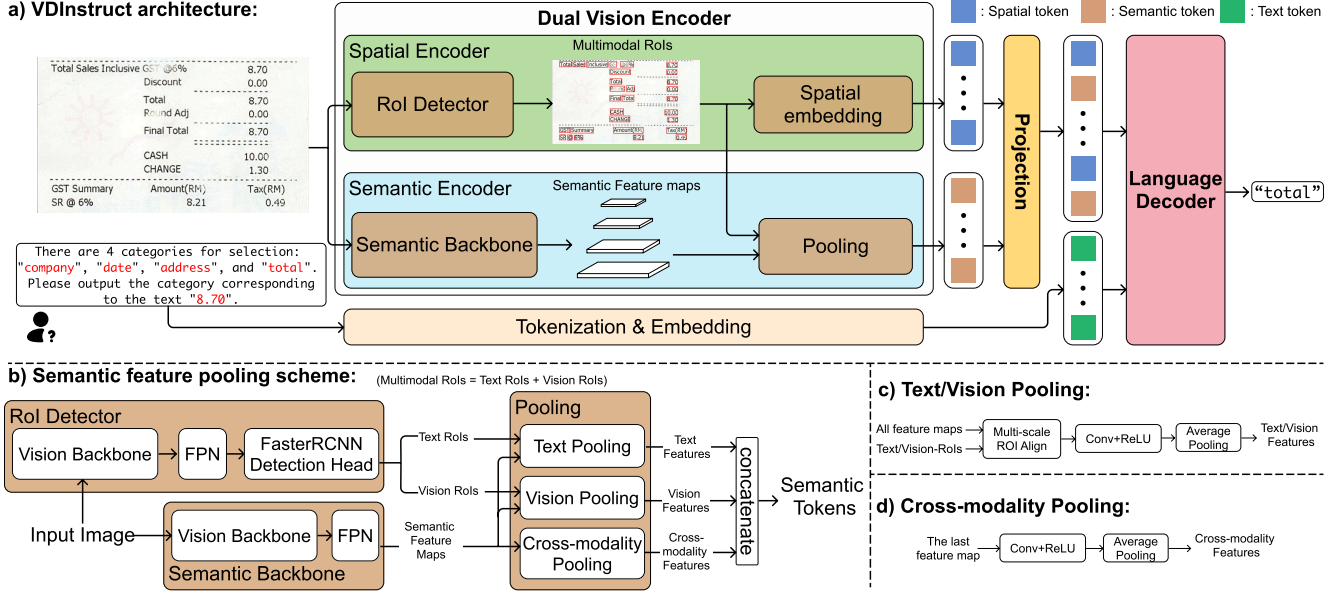


Figure 2. Overview of VDIInSTRUCT. (a) The model architecture. The core module is the dual vision encoder: a spatial encoder to detect text/vision regions (named Multimodal Region of Interest - RoI) and encode them into spatial tokens; a semantic encoder to extract corresponding semantic tokens based on detected RoIs. The details of the semantic feature pooling scheme are shown in (b), (c), and (d).

with a fraction of the parameters. While these works prove KIE benefits from textual, visual, and geometric cues, they still require task-specific fine-tuning and often fail on unseen layouts. Our method tackles this gap by coupling instruction tuning with a token-efficient, layout-aware vision encoder, thereby preserving fine-grained spatial detail while enabling true zero-shot extraction.

3. Methodology

Problem Formulation of Zero-shot KIE We focus on the Semantic Entity Recognition (SER) task, a fundamental task in KIE [17, 47, 49]. We frame zero-shot KIE as a conditional sequence generation problem: given a document image I and a question q specifying a text segment t from the document image with a set of all possible entity labels E_{seen} (e.g., invoice date), the model must output the corresponding entity label $e \in E_{\text{seen}}$ of the given text segment directly. Formally, we learn a mapping: $(I, q(t, E_{\text{seen}})) \mapsto e$. During zero-shot testing, models need to process a set of novel entity labels E_{unseen} , which are not available during training time. This setting requires models not only to localize the given text segment in the input image but also to understand its relation to the unseen entity labels.

3.1. Architecture of VDIInSTRUCT

In processing visual documents, semantic content and spatial layout carry distinct information and require specialized modeling. Most methods rely on a single vision encoder to identify small regions and understand their content, creat-

ing a trade-off: either the page is divided into too many patches, leading to token explosion [13, 23, 50]; or regions are merged excessively, leading to the loss of important layout details [2, 27].

To address this, VDIInSTRUCT adopts a dual vision encoder architecture: a spatial encoder that precisely detects and embeds Multimodal Regions of Interest (ROIs), including textual elements (e.g., words, headers) and visual elements (e.g., figures, charts); and a semantic encoder that extracts visual-textual features from each detected ROIs. By decoupling region localization from feature extraction, each encoder can be trained with objectives tailored to its role, enabling **content-aware tokenization** (i.e., allocating tokens only to informative regions and filtering out redundant areas) that minimizes redundancy while preserving critical layout cues. Fig. 2 shows the overall architecture of VDIInSTRUCT. Our model builds on the standard MLLM architecture, which comprises a vision encoder, a projection layer, and a language decoder, but replaces the single vision encoder with a dual vision encoder (see Fig. 2a). The *spatial encoder* first detects Multimodal ROIs and converts each ROI into a spatial token that encodes its geometry. In parallel, the *semantic encoder* processes those same ROIs to extract fine-grained content features, producing semantic tokens that capture local meaning. We then interleave spatial and semantic tokens by region in reading order, project this structured sequence into the language decoder’s embedding space, and concatenate it with the instruction tokens before decoding.

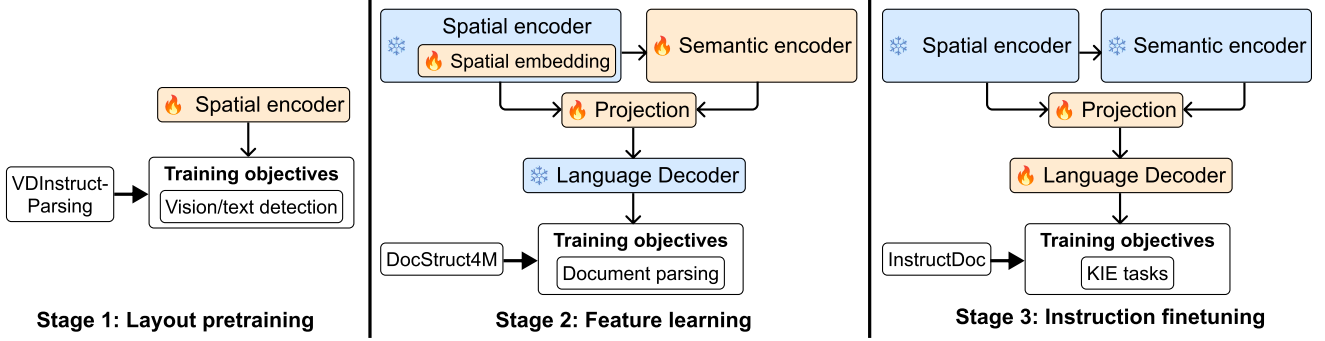


Figure 3. Our proposed 3-stage training paradigm. In **Stage 1**, we train the spatial encoder (without the spatial embedding module) on a detection task using our VDIInstruct-Parsing dataset. After that, we freeze this module and train the remaining part of the vision encoder on document parsing tasks in **Stage 2** to learn the meaningful image tokens. Finally in **Stage 3**, we finetune the projection layers and the language decoder on InstructDoc to enable the instruction-following capability.

The spatial encoder is responsible for detecting and encoding layout-specific regions in document images. As illustrated in Fig. 2a, it contains two key components: a RoI detector, which detects text and vision regions in the input image; and a spatial embedding module constructed with a simple linear layer to project the detected ROIs into spatial tokens. The RoI detector (Fig. 2b) follows the Faster R-CNN architecture [42]: a vision backbone (Swin Transformer v2 [30]) feeds into a Feature Pyramid Network (FPN) [26] to address the scale imbalance between small text regions and larger visual objects. The resulting feature maps are processed by a standard Faster R-CNN detection head to produce N region proposals (ROIs), each classified as a text-ROI or vision-ROI. To preserve global context, we append one additional ROI spanning the entire image, yielding $N + 1$ total regions. Finally, each ROI’s bounding box is projected via a linear layer (the spatial embedding module) into a d -dimensional vector, producing $(N + 1)$ spatial tokens in $\mathbb{R}^{(N+1) \times d}$ that precisely encode the geometry of every detected region.

The semantic encoder extracts fine-grained semantic tokens based on the N multimodal ROIs detected by the spatial encoder. As shown in Fig. 2a, it comprises a semantic backbone and a pooling module. The semantic backbone consists of a vision backbone (Swin Transformer v2 [30]) followed by an FPN [26], which produces multi-scale feature maps. The pooling module takes the multimodal ROIs from the spatial encoder and the feature maps from the semantic backbone. This module contains three parallel sub-modules: *text pooling* for textual ROIs, *vision pooling* for visual ROIs, and *cross-modality pooling* to capture global feature vectors (see Fig. 2b). Fig. 2c shows the text and vision pooling modules, each comprising a multi-scale ROI Align operation, a convolutional layer with ReLU [36] activation, and adaptive average pooling. Each text ROI is pooled into a fixed-size feature map of shape $(s_t \times s_t, d)$,

while each vision ROI is pooled into $(s_v \times s_v, d)$. These are then flattened into sequences of length s_t^2 or s_v^2 , respectively. In addition to region-specific features, we employ a cross-modality pooling module (Fig. 2d) to capture holistic content from the entire image. This global representation is obtained by applying convolution, ReLU [36] activation, and adaptive average pooling to the final backbone feature map, producing a feature map of shape $(s_g \times s_g, d)$, which is then flattened to form s_g^2 cross-modality features. These features help mitigate the effect of imperfect detection and retain comprehensive context across modalities. Finally, all extracted features are concatenated to form the semantic tokens.

3.2. Training

We adopt a three-stage training paradigm (Fig. 3) that incrementally builds VDIInstruct’s abilities, from layout detection \rightarrow semantic understanding \rightarrow instruction following, while allowing each component to specialize and minimizing interference between objectives.

Layout pretraining (Stage 1). The first stage of training aims to teach the spatial encoder to detect multimodal ROIs in document images. Unlike traditional OCR systems, which focus on recognizing and transcribing text, this stage is concerned solely with *region-level detection* (see Appendix A). The training objective at this stage is identical to standard object detection. To support robust pretraining, we construct a dataset named **VDIInstruct-Parsing**, which aggregates document images from seven public sources: AI2D [18], DocLayNet [39], DocBank [21], SciCap [12], ScienceQA [33], KLC [3], and PWC [3]. These datasets span various document types, including scientific papers, academic diagrams, forms, and educational content. For *text annotations*, we leverage existing OCR outputs when available; otherwise, we employ the Azure OCR engine [35]. For *vision annotations*, we annotate rich-

visual areas, such as natural objects, figures, and charts, as visual ROIs (see Appendix B).

Feature learning (Stage 2). This stage aims to extract meaningful visual representations from the detected ROIs by training the semantic encoder and the spatial embedding layer of the spatial encoder. We adapt the document parsing task from DocOwl 1.5 and DocStruct4M dataset [13], formatted in a VQA style with simple parsing instructions. During training, the language decoder is kept frozen, and only the semantic encoder, spatial embedding layer, and projection layer are updated. This allows the model to align visual features with text-space embeddings without affecting the linguistic capacity of the decoder. The training objective combines document structure parsing and fine-grained text localization, encouraging the model to retain content semantics and layout information in its vision tokens.

Instruction tuning (Stage 3). The third stage focuses on instruction fine-tuning, aiming to equip the language decoder with the ability to understand and execute more complex tasks, particularly within the VDU domain. For this purpose, we utilize the InstructDoc dataset [47], which is specifically designed to evaluate the zero-shot capabilities of VLMs on document intelligence tasks. The training data of InstructDoc incorporates approximately 120,000 images, including samples from six KIE datasets (Deepform [3], DocILE [44], PWC [3], KLC [3], SROIE [16], and Wildreceipt [46]), while FUNSD [17] and CORD [37] are held out for zero-shot evaluation. A key advantage of InstructDoc is its provision of a unified format for converting these diverse KIE datasets into a consistent instruction-following structure, directly matching the scope of our work. To specifically isolate the contribution of our vision encoder design to zero-shot KIE performance, we deliberately avoid incorporating large-scale, general-purpose instruction-following datasets often used in VLM training.

4. Experiments

4.1. Training Setup

For the vision backbone, we select Swin Transformer (SwinB-v2) [30] due to its effective balance between performance and computational cost. We also experiment with ResNet-50 [9]. To control token granularity, we use different pooling sizes for each modality to produce a similar number of image tokens as LLaVA 1.5 [28], which uses the same language decoder as VDI_{INSTRUCT}. While larger pooling sizes can help preserve more information, matching LLaVA 1.5’s token count allows us to attribute performance gains to the quality of our vision tokens rather than sheer quantity. Following this heuristic, *text ROIs* are pooled to a (1, 1) size, yielding one token per region; *vision ROIs* to (4, 4), producing 16 tokens; and *cross-modality features* to

(8, 8), contributing 64 high-level contextual tokens. This setting results in approximately 500 image tokens per input, comparable to LLaVA 1.5’s 576. Please see Appendix C.1 for the detailed derivation of token counts.

We plug this vision backbone into the LLaVA framework, utilizing Vicuna v1.5 7B [5] as the large language model. The projection module connecting vision and language features follows the LLaVA v1.5 [28] design (2 linear layers \rightarrow a GeLU activation [10]) but is trained from scratch in our pipeline. Input images are always resized to 1024×1024 , normalized with ImageNet statistics [9] without augmentations. Implementation details and training configurations are provided in Appendix C.2.

4.2. Evaluation Metrics

We measure performance at each training stage using established metrics. For ROI detection, we report mean Average Precision (mAP), a standard object-detection metric [25]. For KIE benchmarks, we use the F1 score [17, 49], which balances precision and recall, as our primary metric. We evaluate under two conditions: **In-domain**: test splits of the six KIE datasets used in InstructDoc training (Deepform, DocILE, KLC, PWC, SROIE, Wildreceipt). **Out-of-domain**: held-out FUNSD and CORD datasets to assess zero-shot generalization. This setup lets us quantify both supervised accuracy and true zero-shot performance.

4.3. Findings

Spatial encoder achieves high multimodal ROI detection accuracy. Since the spatial encoder is responsible for capturing document structure via multimodal ROIs, its detection accuracy is the driving force for preserving layout information and underpins VDI_{INSTRUCT}’s overall performance. We quantify this capability using mean Average Precision (mAP), the standard object-detection metric. With SwinB-v2 [30] as the backbone, our ROI detector achieves an mAP of 0.611 and an AP@50 of 0.818, showing strong localization accuracy. Class-specific APs—0.605 for text regions and 0.618 for vision regions—confirm balanced performance across modalities. Please see Tab. 3 for more ablation studies on different vision backbone choices, and Appendix D for the qualitative results of ROI detection.

VDI_{INSTRUCT} achieves high accuracy on KIE benchmarks. Tab. 1 reports KIE results for VDI_{INSTRUCT} and our selected baselines. We restrict comparisons to models with publicly available pretrained checkpoints before instruction fine-tuning, ensuring that performance differences reflect the vision encoder design rather than extra instruction-tuning data. We fine-tune 3 models, including DocOwl 1.5 [13], LLaVA 1.5 [28], and Qwen2VL [50], on the same InstructDoc dataset used to train VDI_{INSTRUCT}. BLIP-2 [20] and InstructDr [47] are imported from InstructDoc Tanaka *et al.* [47]. Additionally, we include reference

Table 1. Evaluation (F1 scores and image tokens) on KIE datasets. "V", "T", and "L" denote input modalities: image, text, and bounding boxes (text and bounding boxes are extracted by an external OCR tool), respectively. Models with "*" are imported from InstructDoc [47]. VDIINSTRUCT shows the SOTA results while significantly reducing the image tokens.

Model	#Param	Modal	In-domain							Out-of-domain (zero-shot)			Overall Avg
			Deepform	DocLE	KLC	PWC	SROIE	Wildreceipt	Avg	FUNSD	CORD	Avg	
LLaVAR [57]	13.3B	V	0.7	0.0	0.1	0.6	0.2	0.0	0.3	0.6	0.0	0.3	0.3
MiniGPT-v2 [4]	7B	V	6.3	5.2	0.3	15.3	49.8	0.3	12.9	4.4	18.9	11.7	12.6
InstructBLIP [6]	3.4B	V	0.0	0.0	0.0	0.9	0.0	0.0	0.2	0.0	0.0	0.0	0.1
BLIP-2 [20]	3.4B	V	0.0	0.0	0.0	0.0	0.0	0.0	0.0	0.0	0.0	0.0	0.0
Monkey [23]	9.8B	V	19.0	1.3	19.4	11.2	70.5	1.8	20.5	13.1	10.4	11.8	18.3
TextMonkey [29]	9.7B	V	19.3	0.2	3.2	14.2	34.5	1.1	12.1	8.0	0.0	4.0	10.1
DocLayLLM [24]	8B	VT	60.4	13.8	72.9	17.1	89.0	48.8	50.3	19.9	48.9	34.4	46.4
LLaVA 1.5 [28]	7.3B	V	34.8	13.7	41.8	14.3	71.0	12.9	31.4	10.9	31.2	21.1	28.8
DocOwl 1.5 [13]	8.1B	V	36.2	5.5	23.3	19.7	57.5	5.0	24.5	20.6	12.6	16.6	22.6
Finetuned on InstructDoc:													
BLIP-2 [20]*	3.4B	VT	-	-	-	-	-	-	-	26.0	33.8	29.9	-
InstructDr [47]*	3.4B	VT	-	-	-	-	-	-	-	38.2	46.0	42.1	-
Qwen2VL [50]	7B	V	49.1	21.7	22.1	4.1	25.0	22.5	24.1	30.3	36.2	33.3	26.4
LLaVA 1.5 [28]	7.3B	V	80.1	71.3	86.3	20.2	99.8	82.8	73.4	40.1	60.1	50.1	67.6
DocOwl 1.5 [13]	8.1B	V	96.3	78.7	86.6	20.0	99.8	85.6	77.8	45.5	57.8	51.7	71.3
VDIINSTRUCT	7.2B	V	93.3	74.2	86.6	20.0	99.9	83.1	76.2	50.7	63.6	57.2	71.4
Number of image tokens:													
DocOwl 1.5 [13]	8.1B	V	1799	1802	1799	1799	1767	1508	1746	1799	1868	1834	1768
VDIINSTRUCT	7.2B	V	808	488	219	1027	377	282	534	488	192	340	485
			(2.2 ×↓)	(3.7 ×↓)	(8.2 ×↓)	(1.8 ×↓)	(4.7 ×↓)	(5.3 ×↓)	(3.3 ×↓)	(3.7 ×↓)	(9.7 ×↓)	(5.4 ×↓)	(3.6 ×↓)

models trained with their own instruction-following data to showcase the performance without fine-tuning on InstructDoc, such as MiniGPT-v2 [4] and Monkey [23]. Testing on the in-domain setting (Tab. 1), VDIINSTRUCT achieves an average F1 of 76.2, ranking second-best on four out of six datasets and achieving the best score on KLC and SROIE. Although VDIINSTRUCT slightly reduces accuracy on supervised datasets, it achieves notable improvements in out-of-domain performance, suggesting enhanced generalization for KIE tasks. To be specific, in the zero-shot setting, our model achieves SOTA results with an average F1 of 57.2, outperforming all other baselines by a large margin. Compared to DocOwl 1.5, VDIINSTRUCT outperforms this model by a significant gap, **+5.5** points. Our model also consistently beats Qwen2VL and LLaVA 1.5 on all datasets. Compared to LLaVA 1.5, which shares the same language decoder but uses a different vision pipeline, VDIINSTRUCT shows a performance gain of **+7.1** points, indicating the efficiency of our dual vision encoder design. Furthermore, despite not using text recognition systems, VDIINSTRUCT surpasses both OCR-free (LLaVA 1.5, DocOwl 1.5, Qwen2VL) and OCR-based models (InstructDr). Finally, our model achieves the best overall average scores, 71.4 points. In Fig. 4, we demonstrate the qualitative results of VDIINSTRUCT and its counterparts on zero-shot samples. These findings highlight the effectiveness of our dual vision encoder and layout-aware training in achieving robust KIE performance.

Efficient image tokenization: 3.6× fewer tokens without accuracy trade-off. Beyond accuracy, we also measure how efficiently each model encodes document images by reporting the **average number of image tokens** per doc-

Table 2. F1 scores of VDIINSTRUCT when using different semantic token modality combinations. CROSS, TEXT, VISION correspond to cross-modality, textual-modality, and visual-modality semantic tokens, respectively. VDIINSTRUCT achieves the best performance on KIE benchmarks when using all semantic tokens (Cross+Text+Vision). We add LLaVA 1.5 for a better comparison.

Modality	Avg (ID)	Avg (OOD)	Overall
Cross	71.2	55.3	67.2
Cross+Vision	71.2	57.1	67.6
Cross+Text	76.1	56.3	71.2
Cross+Text+Vision	76.2	57.2	71.4
LLaVA 1.5 [28]	73.4	50.1	67.6

ument. Efficiency is critical: every extra token incurs risks overflowing the decoder’s limited context window, directly impacting computational cost and scalability [55]. In Fig. 1 and Tab. 1, VDIINSTRUCT produces approximately 500 image tokens per document on average, which is about **3.6** times fewer than DocOwl 1.5. Despite this significant reduction, VDIINSTRUCT achieves SOTA performance across KIE datasets, demonstrating that our dual-encoder design effectively preserves essential semantic and layout information without generating redundant tokens. Compared to LLaVA 1.5, which shares the same architecture for the language decoder and projection layer with VDIINSTRUCT, our model consistently achieves better KIE performance despite producing a similar number of image tokens. This result suggests that while other counterparts scale image tokens with input resolution, VDIINSTRUCT scales tokens with the document’s content, enabling more effective and efficient image encoding.

CORD:



Categories: "menu_name", "menu_id", "menu_unitprice", "menu_quantity", "menu_discountprice", "menu_price", "menu_price_discount_applied", "menu_whether_price_tax_includes", "menu_etc", "submenu_name", "submenu_unitprice", "submenu_quantity", "submenu_price", "submenu_etc", "voidmenu_price", "voidmenu_price", "subtotal_price", "subtotal_discount_price", "subtotal_service_price", "subtotal_chargeprice", "subtotal_tax_price", "subtotal_etc", "total_price", "total_etc", "total_cashprice", "total_changeprice", "total_creditcardprice", "total_emoneyprice", "total_menutype_count", and "total_menuquantity_count".

Kindly provide me with the category of the text "6.000".

Groundtruth:	Docowl1.5:	LLaVA1.5:	VDInstruct:
"menu_price"	"subtotal_price"	"submenu_price"	"menu_price"
	✗	✗	✓



There are 30 categories for selection: "menu_name", "menu_id", "menu_unitprice", "menu_quantity", "menu_discountprice", "menu_price", "menu_price_discount_applied", "menu_whether_price_tax_includes", "menu_etc", "submenu_name", "submenu_unitprice", "submenu_quantity", "submenu_price", "submenu_etc", "voidmenu_name", "voidmenu_price", "subtotal_price", "subtotal_discount_price", "subtotal_service_price", "subtotal_chargeprice", "subtotal_tax_price", "subtotal_etc", "total_price", "total_etc", "total_cashprice", "total_changeprice", "total_creditcardprice", "total_emoneyprice", "total_menutype_count", and "total_menuquantity_count".

Please output the category corresponding to the text "145,900". Your answer contains only the category, and you should not use verb.

Groundtruth:	Docowl1.5:	LLaVA1.5:	VDInstruct:
"total_price"	"total_cashprice"	"total_cashprice"	"total_price"
	✗	✗	✓

FUNSD:

RTT, GEN, RPDN OFFICE Fax: (614) 466-5087 Dec 10 '98 17:46 P.01

Attorney General
Betty D. Montgomery

CONFIDENTIAL FACSIMILE
TRANSMISSION COVER SHEET
FAX NO. (614) 466-5087

TO: Governor Bentley
FAX NUMBER: (614) 315-7292 PHONE NUMBER: (614) 315-7343
DATE: 12/10/98
NUMBER OF PAGES INCLUDING COVER SHEET: 3
SENDER/PHONE NUMBER: June Form for Data Bureau (614) 466-8080
SPECIAL INSTRUCTIONS:

IF YOU DO NOT RECEIVE ANY OF THE PAGES PROPERLY,
PLEASE CONTACT SENDER
AS SOON AS POSSIBLE

NOTE: THIS MESSAGE IS INTENDED ONLY FOR THE USE OF THE INDIVIDUAL OR ENTITY TO WHOM IT IS ADDRESSED AND MAY CONTAIN INFORMATION THAT IS PRELIMINARY, CONFIDENTIAL, AND EXEMPT FROM DISCLOSURE UNDER APPLICABLE LAW. If the sender of this message is not the intended recipient or the addressee or agent authorized to receive the message on the intended recipient's behalf, you are hereby notified that any dissemination, distribution, copying, or forwarding of this communication is strictly prohibited. If you have received this communication in error, please notify us immediately by telephone and destroy the original message to us at the address below via the U.S. Postal Service. Thank you for your cooperation.

State Office Tower / 50 East Broad Street / Columbus, Ohio 43215-0428
www.governor.ohio.gov
An Equal Opportunity Employer

82092117

Please tell me the category of the text "NOTE" to select from following classes: "title", "key", "value", and "other".

Groundtruth:	Docowl1.5:	LLaVA1.5:	VDInstruct:
"key"	"value"	"other"	"key"
	✗	✗	✓

Figure 4. Qualitative results on the out-of-domain datasets. The red bounding boxes indicate the text segments mentioned in the questions. VDINSTRUCT can correctly predict the labels of the selected text segments, whereas DocOwl 1.5 and LLaVA 1.5 cannot.

Complementary token modalities deliver best performance. We also investigate the impact of different modalities of the *semantic* tokens produced by the dual vision encoder. In Tab. 2, we start with using only cross-modality tokens (CROSS), then gradually add textual-modality (TEXT) and visual-modality tokens (VISUAL). In this experiment, we do not re-train the entire model but simply ablate out the corresponding tokens in each setting during the inference. We use LLaVA 1.5 for reference since it shares the same language decoder (Vicuna v1.5 7B) with our model. With only cross-modality tokens, VDINSTRUCT underperforms its counterpart, LLaVA 1.5, although it performs better on out-of-domain benchmarks. This is reasonable since image tokens consumed by VDINSTRUCT in this case are much smaller than LLaVA 1.5 (64 compared to 576). When adding visual-modality tokens to the vision encoder’s outputs, VDINSTRUCT achieves the same F1 score with LLaVA 1.5 by increasing its zero-shot accuracy by 1.8 points. Pairing cross-modality and text-modality tokens boosts VDINSTRUCT’s performance by a significant gap, from 67.2 to 71.2-underscoring the critical role of fine-grained text segments in document images. Finally, the combination of all token modalities achieves the highest scores across all benchmarks, as reported in Tab. 1. These results demonstrate that the different types of semantic to-

kens are complementary; each modality contributes unique information that, when combined, yields the strongest overall performance.

Spatial tokens contribute meaningfully to KIE performance. To assess the contribution of spatial tokens, we conduct an ablation study by removing them from the input to the language decoder while keeping all other components intact. As shown in Tab. 4, excluding spatial tokens leads to a performance drop in both in-domain and out-of-domain settings. Specifically, the overall F1 score decreases from 71.4 to 70.7, with a more pronounced decline in zero-shot (out-of-domain) performance. This highlights the role of spatial tokens in encoding layout-specific cues that complement semantic features and support robust generalization across document types.

Stronger vision backbone improves detection and zero-shot KIE. To quantify the effect of vision backbone selection on ROI detection and KIE performance, we conducted an ablation comparing ResNet-50 [9] and SwinB-v2 [30] as the shared backbone for both spatial and semantic encoders. As Tab. 3 shows, SwinB-v2 dramatically improves ROI localization, raising mAP from 0.443 to 0.611 and AP@50 from 0.614 to 0.818, while also delivering balanced text and vision APs. These gains carry over to downstream key information extraction: after fine-tuning on Instruct-

Table 3. Comparison of detection performance between ResNet-50 and Swin-B v2 backbones. Swin-B v2 achieves better results across every evaluation metric.

Backbone	AP	AP50	AP _{text}	AP _{vision}
ResNet-50 [9]	0.443	0.614	0.561	0.325
SwinB-v2 [30]	0.611	0.818	0.605	0.618

Table 5. KIE benchmark comparison between different vision backbones. VDIINSTRUCT performs best with SwinB-v2 as backbones for both spatial and semantic encoders.

Backbone	Deepform	DocILE	KLC	PWC	SROIE	WR	Avg (ID)	FUNSD	CORD	Avg (OOD)	Overall Avg
ResNet-50 [9]	79.7	63.8	84.4	20.0	99.9	78.0	71.0	38.0	63.8	50.9	66.0
SwinB-v2 [30]	93.3	74.2	86.4	20.0	99.9	83.1	76.2	50.7	63.6	57.2	71.4

Doc, as shown in Tab. 5, VDIINSTRUCT with SwinB-v2 achieves an in-domain F1 of 76.2 and an out-of-domain F1 of 57.2—+5.2 and +5.7 points higher than the ResNet-50 variant—resulting in an overall F1 of 71.4 versus 66.0.

5. Conclusion

In this paper, we introduce VDIINSTRUCT, a multimodal LLM for Key Information Extraction that decouples spatial layout detection and semantic feature extraction via a dual-vision encoder. By leveraging *content-aware tokenization*—allocating tokens to the most informative regions—and a three-stage training paradigm (layout pre-training, feature learning, and instruction tuning), VDIINSTRUCT shows greater vision encoding efficiency while achieving strong generalization in zero-shot settings and maintaining SOTA performance on KIE tasks.

Despite these strong results on KIE benchmarks, VDIINSTRUCT’s performance depends heavily on the accuracy of the spatial encoder’s predictions. Incorrect or overlapping bounding box detections may lead to redundant tokens and affect overall performance. Future work could remedy this problem by expanding the training dataset to include more diverse document types and resolutions to improve the model’s robustness further.

References

- [1] Srikanth Appalaraju, Bhavan Jasani, Bhargava Urala Kota, Yusheng Xie, and R Manmatha. Docformer: End-to-end transformer for document understanding. In *Proceedings of the IEEE/CVF international conference on computer vision*, pages 993–1003, 2021. 1, 2
- [2] Jinze Bai, Shuai Bai, Shusheng Yang, Shijie Wang, Sinan Tan, Peng Wang, Junyang Lin, Chang Zhou, and Jingren Zhou. Qwen-vl: A versatile vision-language model for understanding, localization. *Text Reading, and Beyond*, 2, 2023. 2, 3
- [3] Łukasz Borchmann, Michał Pietruszka, Tomasz Stanisławek, Dawid Jurkiewicz, Michał Turski, Karolina Szyndler,

Table 4. F1 scores of VDIINSTRUCT with and without spatial tokens. The performance of VDIINSTRUCT drops on both in-domain and out-of-domain when excluding spatial tokens.

Configuration	Avg (ID)	Avg (OOD)	Overall Avg
w/ spatial tokens	76.2	57.2	71.4
w/o spatial tokens	75.8	55.2	70.7

and Filip Graliński. Due: End-to-end document understanding benchmark. In *Thirty-fifth Conference on Neural Information Processing Systems Datasets and Benchmarks Track (Round 2)*, 2021. 4, 5

- [4] Jun Chen, Deyao Zhu, Xiaoqian Shen, Xiang Li, Zechun Liu, Pengchuan Zhang, Raghuraman Krishnamoorthi, Vikas Chandra, Yunyang Xiong, and Mohamed Elhoseiny. Minigpt-v2: large language model as a unified interface for vision-language multi-task learning. *arXiv preprint arXiv:2310.09478*, 2023. 6
- [5] Wei-Lin Chiang, Zhuohan Li, Zi Lin, Ying Sheng, Zhanghao Wu, Hao Zhang, Lianmin Zheng, Siyuan Zhuang, Yonghao Zhuang, Joseph E. Gonzalez, Ion Stoica, and Eric P. Xing. Vicuna: An open-source chatbot impressing gpt-4 with 90%* chatgpt quality, 2023. 5
- [6] W Dai, J Li, D Li, AMH Tiong, J Zhao, W Wang, B Li, P Fung, and S Hoi. Instructblip: towards general-purpose vision-language models with instruction tuning. *arxiv. Preprint posted online on June, 15:2023*, 2023. 6
- [7] Hao Feng, Qi Liu, Hao Liu, Jingqun Tang, Wengang Zhou, Houqiang Li, and Can Huang. Docpedia: Unleashing the power of large multimodal model in the frequency domain for versatile document understanding. *Science China Information Sciences*, 67(12):1–14, 2024. 2
- [8] Jiuxiang Gu, Jason Kuen, Vlad I Morariu, Handong Zhao, Rajiv Jain, Nikolaos Barmpalios, Ani Nenkova, and Tong Sun. Unidoc: Unified pretraining framework for document understanding. *Advances in Neural Information Processing Systems*, 34:39–50, 2021. 1
- [9] Kaiming He, Xiangyu Zhang, Shaoqing Ren, and Jian Sun. Deep residual learning for image recognition. In *Proceedings of the IEEE conference on computer vision and pattern recognition*, pages 770–778, 2016. 5, 7, 8
- [10] Dan Hendrycks and Kevin Gimpel. Gaussian error linear units (gelus). *arXiv preprint arXiv:1606.08415*, 2016. 5
- [11] Wenyi Hong, Weihang Wang, Qingsong Lv, Jiazhang Xu, Wenmeng Yu, Junhui Ji, Yan Wang, Zihan Wang, Yuxiao Dong, Ming Ding, et al. Cogagent: A visual language model for gui agents. In *Proceedings of the IEEE/CVF Conference on Computer Vision and Pattern Recognition*, pages 14281–14290, 2024. 2

- [12] Ting-Yao Hsu, C Lee Giles, and Ting-Hao Huang. SciCap: Generating captions for scientific figures. In *Findings of the Association for Computational Linguistics: EMNLP 2021*, pages 3258–3264, Punta Cana, Dominican Republic, 2021. Association for Computational Linguistics. 4
- [13] Anwen Hu, Haiyang Xu, Jiabo Ye, Ming Yan, Liang Zhang, Bo Zhang, Ji Zhang, Qin Jin, Fei Huang, and Jingren Zhou. mPLUG-DocOwl 1.5: Unified structure learning for OCR-free document understanding. *Findings of the Association for Computational Linguistics: EMNLP 2024*, pages 3096–3120, 2024. 1, 2, 3, 5, 6
- [14] Edward J Hu, Yelong Shen, Phillip Wallis, Zeyuan Allen-Zhu, Yanzhi Li, Shean Wang, Lu Wang, Weizhu Chen, et al. Lora: Low-rank adaptation of large language models. *ICLR*, 1(2):3, 2022. 2
- [15] Yupan Huang, Tengchao Lv, Lei Cui, Yutong Lu, and Furu Wei. Layoutlmv3: Pre-training for document ai with unified text and image masking. In *Proceedings of the 30th ACM international conference on multimedia*, pages 4083–4091, 2022. 2, 1
- [16] Zheng Huang, Kai Chen, Jianhua He, Xiang Bai, Dimosthenis Karatzas, Shijian Lu, and CV Jawahar. Icdar2019 competition on scanned receipt ocr and information extraction. In *2019 International Conference on Document Analysis and Recognition (ICDAR)*, pages 1516–1520. IEEE, 2019. 5
- [17] Guillaume Jaume, Hazim Kemal Ekenel, and Jean-Philippe Thiran. Funsd: A dataset for form understanding in noisy scanned documents. In *2019 International Conference on Document Analysis and Recognition Workshops (ICDARW)*, pages 1–6. IEEE, 2019. 3, 5
- [18] Aniruddha Kembhavi, Mike Salvato, Eric Kolve, Minjoon Seo, Hannaneh Hajishirzi, and Ali Farhadi. A diagram is worth a dozen images. In *Computer Vision—ECCV 2016: 14th European Conference, Amsterdam, The Netherlands, October 11–14, 2016, Proceedings, Part IV 14*, pages 235–251. Springer, 2016. 4
- [19] Geewook Kim, Teakgyu Hong, Moonbin Yim, Jinyoung Park, Jinyeong Yim, Wonseok Hwang, Sangdoo Yun, Dongyoon Han, and Seunghyun Park. Donut: Document understanding transformer without ocr. *arXiv preprint arXiv:2111.15664*, 7(15):2, 2021. 1
- [20] Junnan Li, Dongxu Li, Silvio Savarese, and Steven Hoi. Blip-2: Bootstrapping language-image pre-training with frozen image encoders and large language models. In *International conference on machine learning*, pages 19730–19742. PMLR, 2023. 5, 6
- [21] Minghao Li, Yiheng Xu, Lei Cui, Shaohan Huang, Furu Wei, Zhoujun Li, and Ming Zhou. DocBank: A benchmark dataset for document layout analysis. In *Proceedings of the 28th International Conference on Computational Linguistics*, pages 949–960, Barcelona, Spain (Online), 2020. International Committee on Computational Linguistics. 4
- [22] Peizhao Li, Jiuxiang Gu, Jason Kuen, Vlad I Morariu, Handong Zhao, Rajiv Jain, Varun Manjunatha, and Hongfu Liu. Selfdoc: Self-supervised document representation learning. In *Proceedings of the IEEE/CVF Conference on Computer Vision and Pattern Recognition*, pages 5652–5660, 2021. 2, 1
- [23] Zhang Li, Biao Yang, Qiang Liu, Zhiyin Ma, Shuo Zhang, Jingxu Yang, Yabo Sun, Yuliang Liu, and Xiang Bai. Monkey: Image resolution and text label are important things for large multi-modal models. In *proceedings of the IEEE/CVF conference on computer vision and pattern recognition*, pages 26763–26773, 2024. 3, 6
- [24] Wenhui Liao, Jiapeng Wang, Hongliang Li, Chengyu Wang, Jun Huang, and Lianwen Jin. Doclaylm: An efficient and effective multi-modal extension of large language models for text-rich document understanding. *arXiv preprint arXiv:2408.15045*, 2024. 6
- [25] Tsung-Yi Lin, Michael Maire, Serge Belongie, James Hays, Pietro Perona, Deva Ramanan, Piotr Dollár, and C Lawrence Zitnick. Microsoft coco: Common objects in context. In *Computer vision—ECCV 2014: 13th European conference, zurich, Switzerland, September 6–12, 2014, proceedings, part v 13*, pages 740–755. Springer, 2014. 5
- [26] Tsung-Yi Lin, Piotr Dollár, Ross Girshick, Kaiming He, Bharath Hariharan, and Serge Belongie. Feature pyramid networks for object detection. In *Proceedings of the IEEE conference on computer vision and pattern recognition*, pages 2117–2125, 2017. 4
- [27] Haotian Liu, Chunyuan Li, Qingyang Wu, and Yong Jae Lee. Visual instruction tuning. *Advances in neural information processing systems*, 36:34892–34916, 2023. 2, 3
- [28] Haotian Liu, Chunyuan Li, Yuheng Li, and Yong Jae Lee. Improved baselines with visual instruction tuning. In *Proceedings of the IEEE/CVF Conference on Computer Vision and Pattern Recognition*, pages 26296–26306, 2024. 5, 6, 2
- [29] Yuliang Liu, Biao Yang, Qiang Liu, Zhang Li, Zhiyin Ma, Shuo Zhang, and Xiang Bai. Textmonkey: An ocr-free large multimodal model for understanding document. *arXiv preprint arXiv:2403.04473*, 2024. 6
- [30] Ze Liu, Han Hu, Yutong Lin, Zhuliang Yao, Zhenda Xie, Yixuan Wei, Jia Ning, Yue Cao, Zheng Zhang, Li Dong, et al. Swin transformer v2: Scaling up capacity and resolution. In *Proceedings of the IEEE/CVF conference on computer vision and pattern recognition*, pages 12009–12019, 2022. 4, 5, 7, 8
- [31] Ilya Loshchilov and Frank Hutter. Sgdr: Stochastic gradient descent with warm restarts. *arXiv preprint arXiv:1608.03983*, 2016. 2
- [32] Ilya Loshchilov and Frank Hutter. Decoupled weight decay regularization. *arXiv preprint arXiv:1711.05101*, 2017. 2
- [33] Pan Lu, Swaroop Mishra, Tanglin Xia, Liang Qiu, Kai-Wei Chang, Song-Chun Zhu, Oyvind Tafjord, Peter Clark, and Ashwin Kalyan. Learn to explain: Multimodal reasoning via thought chains for science question answering. *Advances in Neural Information Processing Systems*, 35:2507–2521, 2022. 4
- [34] Minesh Mathew, Dimosthenis Karatzas, R Manmatha, and CV Jawahar. Docvqa: a dataset for vqa on document images. corr abs/2007.00398 (2020). *arXiv preprint arXiv:2007.00398*, 2(3), 2020. 2
- [35] Microsoft. Azure Cognitive Services: Optical Character Recognition (OCR). <https://learn.microsoft.com/en-us/azure/cognitive->

- [services/computer-vision/](#), 2023. Accessed: 2025-05-05. 4
- [36] Vinod Nair and Geoffrey E Hinton. Rectified linear units improve restricted boltzmann machines. In *Proceedings of the 27th international conference on machine learning (ICML-10)*, pages 807–814, 2010. 4
- [37] Seunghyun Park, Seung Shin, Bado Lee, Junyeop Lee, Jaeheung Surh, Minjoon Seo, and Hwalsuk Lee. Cord: a consolidated receipt dataset for post-ocr parsing. In *Workshop on Document Intelligence at NeurIPS 2019*, 2019. 5
- [38] Adam Paszke, Sam Gross, Soumith Chintala, Gregory Chanan, Edward Yang, Zachary DeVito, Zeming Lin, Alban Desmaison, Luca Antiga, and Adam Lerer. Automatic differentiation in pytorch. In *NIPS-W*, 2017. 2
- [39] Birgit Pfitzmann, Christoph Auer, Michele Dolfi, Ahmed S Nassar, and Peter Staar. Doclaynet: A large human-annotated dataset for document-layout segmentation. In *Proceedings of the 28th ACM SIGKDD conference on knowledge discovery and data mining*, pages 3743–3751, 2022. 4
- [40] Rafał Powalski, Łukasz Borchmann, Dawid Jurkiewicz, Tomasz Dwojak, Michał Pietruszka, and Gabriela Pałka. Going full-tilt boogie on document understanding with text-image-layout transformer. In *Document Analysis and Recognition-ICDAR 2021: 16th International Conference, Lausanne, Switzerland, September 5–10, 2021, Proceedings, Part II 16*, pages 732–747. Springer, 2021. 1
- [41] Jeff Rasley, Samyam Rajbhandari, Olatunji Ruwase, and Yuxiong He. Deepspeed: System optimizations enable training deep learning models with over 100 billion parameters. In *Proceedings of the 26th ACM SIGKDD international conference on knowledge discovery & data mining*, pages 3505–3506, 2020. 2
- [42] Shaoqing Ren, Kaiming He, Ross Girshick, and Jian Sun. Faster r-cnn: Towards real-time object detection with region proposal networks. *Advances in neural information processing systems*, 28, 2015. 4
- [43] Alexander Rombach and Peter Fettke. Deep learning based key information extraction from business documents: Systematic literature review. *arXiv preprint arXiv:2408.06345*, 2024. 2
- [44] Štěpán Šimsa, Milan Šulc, Michal Uříčář, Yash Patel, Ahmed Hamdi, Matěj Kocián, Matyáš Skalický, Jiří Matas, Antoine Doucet, Mickaël Coustaty, et al. Docile benchmark for document information localization and extraction. In *International Conference on Document Analysis and Recognition*, pages 147–166. Springer, 2023. 5
- [45] Amanpreet Singh, Vivek Natarajan, Meet Shah, Yu Jiang, Xinlei Chen, Dhruv Batra, Devi Parikh, and Marcus Rohrbach. Towards vqa models that can read. In *Proceedings of the IEEE/CVF conference on computer vision and pattern recognition*, pages 8317–8326, 2019. 2
- [46] Hongbin Sun, Zhanghui Kuang, Xiaoyu Yue, Chenhao Lin, and Wayne Zhang. Spatial dual-modality graph reasoning for key information extraction. *arXiv preprint arXiv:2103.14470*, 2021. 5
- [47] Ryota Tanaka, Taichi Iki, Kyosuke Nishida, Kuniko Saito, and Jun Suzuki. Instructdoc: A dataset for zero-shot generalization of visual document understanding with instructions. In *Proceedings of the AAAI conference on artificial intelligence*, pages 19071–19079, 2024. 2, 3, 5, 6
- [48] Dongsheng Wang, Natraj Raman, Mathieu Sibue, Zhiqiang Ma, Petr Babkin, Simerjot Kaur, Yulong Pei, Armineh Nourbakhsh, and Xiaomo Liu. Docllm: A layout-aware generative language model for multimodal document understanding. *Proceedings of the 62nd Annual Meeting of the Association for Computational Linguistics (Volume 1: Long Papers)*, pages 8529–8548, 2024. 1, 2
- [49] Hao Wang, Xiahua Chen, Rui Wang, and Chenhui Chu. Vision-enhanced semantic entity recognition in document images via visually-asymmetric consistency learning. In *Proceedings of the 2023 Conference on Empirical Methods in Natural Language Processing*, pages 15718–15731, 2023. 3, 5
- [50] Peng Wang, Shuai Bai, Sinan Tan, Shijie Wang, Zhihao Fan, Jinze Bai, Keqin Chen, Xuejing Liu, Jialin Wang, Wenbin Ge, et al. Qwen2-vl: Enhancing vision-language model’s perception of the world at any resolution. *arXiv preprint arXiv:2409.12191*, 2024. 2, 3, 5, 6
- [51] Yiheng Xu, Minghao Li, Lei Cui, Shaohan Huang, Furu Wei, and Ming Zhou. Layoutlm: Pre-training of text and layout for document image understanding. In *Proceedings of the 26th ACM SIGKDD international conference on knowledge discovery & data mining*, pages 1192–1200, 2020. 1, 2
- [52] Yang Xu, Yiheng Xu, Tengchao Lv, Lei Cui, Furu Wei, Guoxin Wang, Yijuan Lu, Dinei Florencio, Cha Zhang, Wanxiang Che, et al. Layoutlmv2: Multi-modal pre-training for visually-rich document understanding. In *Proceedings of the 59th Annual Meeting of the Association for Computational Linguistics and the 11th International Joint Conference on Natural Language Processing (Volume 1: Long Papers)*, pages 2579–2591, 2021. 2
- [53] Jiabo Ye, Anwen Hu, Haiyang Xu, Qinghao Ye, Ming Yan, Yuhao Dan, Chenlin Zhao, Guohai Xu, Chenliang Li, Junfeng Tian, Qian Qi, Ji Zhang, and Fei Huang. mPLUG-DocOwl: Modularized multimodal LLM for document understanding. *arXiv preprint arXiv:2307.02499*, 2023. 2
- [54] Jiabo Ye, Anwen Hu, Haiyang Xu, Qinghao Ye, Ming Yan, Guohai Xu, Chenliang Li, Junfeng Tian, Qi Qian, Ji Zhang, Qin Jin, Liang He, Xin Lin, and Fei Huang. UReader: Universal OCR-free visually-situated language understanding with multimodal large language model. In *Findings of the Association for Computational Linguistics: EMNLP 2023*, pages 2841–2858, Singapore, 2023. Association for Computational Linguistics. 2
- [55] Hyungjun Yoon, Biniyam Aschalew Tolera, Taesik Gong, Kimin Lee, and Sung-Ju Lee. By my eyes: Grounding multimodal large language models with sensor data via visual prompting. In *Proceedings of the 2024 Conference on Empirical Methods in Natural Language Processing*, pages 2219–2241, Miami, Florida, USA, 2024. Association for Computational Linguistics. 6
- [56] Yuechen Yu, Yulin Li, Chengquan Zhang, Xiaoqiang Zhang, Zengyuan Guo, Xiameng Qin, Kun Yao, Junyu Han, Errui Ding, and Jingdong Wang. Structxtv2: Masked visual-textual prediction for document image pre-training. *arXiv preprint arXiv:2303.00289*, 2023. 2

- [57] Yanzhe Zhang, Ruiyi Zhang, Jiuxiang Gu, Yufan Zhou, Nedim Lipka, Diyi Yang, and Tong Sun. Llavar: Enhanced visual instruction tuning for text-rich image understanding. *arXiv preprint arXiv:2306.17107*, 2023. [6](#)

VDInstruct: Zero-Shot Key Information Extraction via Content-Aware Vision Tokenization

Supplementary Material

A. VDINSTRUCT vs. existing region-based VDU models

While decoupling region detection from feature extraction has precedent in document understanding literature [8, 22, 40, 51], VDINSTRUCT’s dual-vision encoder differs from prior work in two fundamental ways:

- **OCR-free end-to-end pretrained region detector covering both text and vision regions.** Prior works such as LayoutLM [51], SelfDoc [22], and UDoc [8] employ an external OCR tool to get the Region of Interest (ROI). While this approach can preserve the textual information on the document, it neglects the importance of visual cues. VDINSTRUCT instead builds its spatial encoder from a ResNet-50 or Swin Transformer v2 backbone with an FPN feeding into a Faster R-CNN detection head, which is pretrained end-to-end on a heterogeneous suite of document parsing datasets (Stage 1: Layout pre-training) to directly optimize text- and vision-ROI detection for document layouts, eliminating the need for an external OCR tool. Moreover, our ROI detector in the spatial encoder differs from OCR tools since it only focuses on region localization, not text recognition. Each detected bounding box is then projected via a learned linear layer into a d -dimensional spatial token, enabling region proposals to adapt to document-centric structures rather than generic object categories.
- **Task-aligned semantic encoder rather than pooled region features.** Prior methods extract a single fixed vector per region and concatenate it with text embeddings [8, 22, 40, 51]. VDINSTRUCT’s semantic encoder instead applies a high-resolution backbone (ResNet-50 or Swin Transformer v2 with FPN) to produce multi-scale feature maps, then uses three specialized pooling modules—text pooling for text ROIs, vision pooling for visual ROIs, and cross-modality pooling on the global feature map, each involving multi-scale ROI Align, Conv+ReLU, and adaptive average pooling. Additionally, each detected ROI is pooled into a different size (based on its modality) and flattened to a set of feature vectors rather than one fixed vector per region. The resulting semantic tokens are concatenated to form rich, context-enriched region representations that preserve fine-grained cues (*e.g.*, fonts, textures) and holistic layout information often lost by static ROI-pooled vectors.

These design choices—OCR-free end-to-end trainable region proposals and multi-scale semantic align-

ment—distinguish VDINSTRUCT’s dual-vision encoder from existing region-based document models and underpin its superior performance on both in-domain and zero-shot tasks.

B. VDInstruct-Parsing statistics

From each dataset, we randomly sample up to 50,000 images from the training split to construct a balanced and diverse training set. To maintain data quality and reduce noise, we exclude images that contain more than 1,000 bounding boxes. A similar sampling strategy is applied to create the test set using the original test or validation splits (with a maximum 1,000 samples per dataset). For *vision annotations*, we follow dataset-specific rules: AI2D uses the `blob` attribute, DocBank uses the `figure` class, and DocLayNet uses the `picture` class. For datasets such as SciCap and ScienceQA, where graphical content is often embedded as standalone images, we place these figures on a white background to synthesize a consistent visual region. In cases like KLC and PWC, where predefined visual annotations are lacking, we apply a pretrained document layout analysis model [15] to infer vision regions, taking advantage of the visual similarity between these datasets and the model’s original training data. Tab. 6 and Tab. 7 summarize the sample and bounding box distributions across the seven datasets.

C. Training details of VDINSTRUCT

C.1. The number of image tokens

The total number of image tokens produced by VDINSTRUCT scales with the content of the document rather than its pixel resolution, which helps minimize both token redundancy and information loss. Let N_t and N_v denote the number of text ROIs and vision ROIs, respectively. Then, the total number of detected regions is $N = N_t + N_v$. The number of spatial tokens is:

$$N_{\text{spatial_tokens}} = N_t + N_v + 1 \quad (1)$$

where the one extra token corresponds to the bounding box covering the entire image.

Using pooling, each text ROI contributes s_t^2 features (tokens) and each vision ROI contributes s_v^2 features, while the global branch adds s_g^2 cross-modality features. Thus, the total number of semantic tokens is given by:

$$N_{\text{semantic_tokens}} = N_t \cdot s_t^2 + N_v \cdot s_v^2 + s_g^2 \quad (2)$$

Table 6. Sample distribution in the VDIInstruct-Parsing dataset across training and test sets.

	AI2D	DocLayNet	DocBank	SciCap	ScienceQA	KLC	PWC	Total
Train	3,921	48,179	49,301	49,997	6,218	1,729	208	159,553
Test	982	975	990	1,000	1,000	440	63	5,450

Table 7. Bounding box statistics in the VDIINSTRUCT-Parsing dataset.

	Text Boxes	Vision Boxes	Total
Train	46,403.1K	113.1K	46,516.2K
Test	983.0K	7.6K	990.6K

Finally, the total number of image tokens, denoted as $N_{\text{image_tokens}}$, is:

$$N_{\text{image_tokens}} = N_{\text{spatial_tokens}} + N_{\text{semantic_tokens}} \\ = (N_t + N_v + 1) + (N_t \cdot s_t^2 + N_v \cdot s_v^2 + s_g^2) \quad (3)$$

This content-aware token allocation allows VDIINSTRUCT to capture all necessary details while keeping the token count low, regardless of the input’s overall resolution.

To determine the appropriate pooling sizes for the semantic encoder, we analytically estimate the number of image tokens generated per input image. We set $s_t = 1$, reflecting the word-level granularity of text RoIs, such that each text RoI is encoded into a single token. To determine s_v and s_g , we analyze the average size of vision RoIs relative to the input image resolution (1024×1024), finding that the average size of vision RoIs is roughly half the image size. Based on this, we set $s_g \approx 2 \cdot s_v$.

Given the average number of RoIs per image ($N_t \approx 293.37$, $N_v \approx 0.71$) (see Tab. 6 and Tab. 7) and the goal of maintaining token efficiency comparable to LLaVA 1.5 [28] (our direct counterpart, which uses 576 vision tokens), we aim to constrain the total number of image tokens to the range $[576 - 100, 576 + 100]$. By solving:

$$476 < (N_t + N_v + 1) + (N_t + (N_v + 4) \cdot s_v^2) \leq 676 \quad (4)$$

we find that $s_v \leq 4$ meets this constraint. To minimize information loss, we select the maximum feasible pooling resolution: $s_v = 4$, and consequently set $s_g = 8$. This results in 1 token per text RoI, 16 tokens per vision RoI, and 64 global tokens per image, balancing efficiency and expressiveness. Please see Fig. 5 for examples on KLC and DocILE datasets.

C.2. Implementation details

All our implementations use PyTorch [38] with Python 3.10. All training uses AdamW [32] with cosine learning rate scheduler [31]. We also leverage DeepSpeed [41] for memory-efficient training. In stage 3, we use the LoRA

techniques [14] for memory-efficient training. For other stages, we use full fine-tuning. Other training details are shown in Tab. 8.

D. Qualitative analysis on RoI detection

Fig. 6 demonstrates the qualitative results of the ROI detector module in the spatial encoder on various document types. Since it is trained on diverse datasets, the ROI detector can detect both word-level text contents and visual objects, such as different types of leaves on the AI2D example. The ROI detector can also process various document types, including receipts in the wild (SROIE sample) or scanned documents (Deepform samples), at different resolutions.

KLC

Charity number: 1138421

ST ANDREW'S CHURCH, ENFIELD

UNAUDITED

TRUSTEES' REPORT AND FINANCIAL STATEMENTS

FOR THE YEAR ENDED 31 DECEMBER 2019

DOCILE

Please Remit To
KMOZ 923 The Moose
110 E. 1st Street
Cedar Rapids IA 52401
563-424-1101

Invoice # 022106
Invoice Total \$1,080.00
Payment Terms: 30 Days

Invoice Month: Aug
Advertiser: The Weber Co. - 563-424-1101
Account: KMOZ-TV, Cedar Rapids
Salesperson: KMOZ-TV, Cedar Rapids
Sales Office: Cedar Rapids, IA 52401

Advertiser: The Weber Co. - 563-424-1101
Flight Dates: 08/01/2019 - 08/31/2019
Salesperson: KMOZ-TV, Cedar Rapids
Sales Office: Cedar Rapids, IA 52401

LINE	CD	SPOT	START DATE	END DATE	SPOTS	SPOT PRICE	TOTAL SPOTS	TOTAL PRICE
1	SPOT	08/01/2019	08/01/2019	08/01/2019	1	\$1,080.00	1	\$1,080.00
2	SPOT	08/02/2019	08/02/2019	08/02/2019	1	\$1,080.00	1	\$1,080.00
3	SPOT	08/03/2019	08/03/2019	08/03/2019	1	\$1,080.00	1	\$1,080.00
4	SPOT	08/04/2019	08/04/2019	08/04/2019	1	\$1,080.00	1	\$1,080.00
5	SPOT	08/05/2019	08/05/2019	08/05/2019	1	\$1,080.00	1	\$1,080.00
6	SPOT	08/06/2019	08/06/2019	08/06/2019	1	\$1,080.00	1	\$1,080.00
7	SPOT	08/07/2019	08/07/2019	08/07/2019	1	\$1,080.00	1	\$1,080.00
8	SPOT	08/08/2019	08/08/2019	08/08/2019	1	\$1,080.00	1	\$1,080.00
9	SPOT	08/09/2019	08/09/2019	08/09/2019	1	\$1,080.00	1	\$1,080.00
10	SPOT	08/10/2019	08/10/2019	08/10/2019	1	\$1,080.00	1	\$1,080.00
11	SPOT	08/11/2019	08/11/2019	08/11/2019	1	\$1,080.00	1	\$1,080.00
12	SPOT	08/12/2019	08/12/2019	08/12/2019	1	\$1,080.00	1	\$1,080.00
13	SPOT	08/13/2019	08/13/2019	08/13/2019	1	\$1,080.00	1	\$1,080.00
14	SPOT	08/14/2019	08/14/2019	08/14/2019	1	\$1,080.00	1	\$1,080.00
15	SPOT	08/15/2019	08/15/2019	08/15/2019	1	\$1,080.00	1	\$1,080.00
16	SPOT	08/16/2019	08/16/2019	08/16/2019	1	\$1,080.00	1	\$1,080.00
17	SPOT	08/17/2019	08/17/2019	08/17/2019	1	\$1,080.00	1	\$1,080.00
18	SPOT	08/18/2019	08/18/2019	08/18/2019	1	\$1,080.00	1	\$1,080.00
19	SPOT	08/19/2019	08/19/2019	08/19/2019	1	\$1,080.00	1	\$1,080.00
20	SPOT	08/20/2019	08/20/2019	08/20/2019	1	\$1,080.00	1	\$1,080.00
21	SPOT	08/21/2019	08/21/2019	08/21/2019	1	\$1,080.00	1	\$1,080.00
22	SPOT	08/22/2019	08/22/2019	08/22/2019	1	\$1,080.00	1	\$1,080.00
23	SPOT	08/23/2019	08/23/2019	08/23/2019	1	\$1,080.00	1	\$1,080.00
24	SPOT	08/24/2019	08/24/2019	08/24/2019	1	\$1,080.00	1	\$1,080.00
25	SPOT	08/25/2019	08/25/2019	08/25/2019	1	\$1,080.00	1	\$1,080.00
26	SPOT	08/26/2019	08/26/2019	08/26/2019	1	\$1,080.00	1	\$1,080.00
27	SPOT	08/27/2019	08/27/2019	08/27/2019	1	\$1,080.00	1	\$1,080.00
28	SPOT	08/28/2019	08/28/2019	08/28/2019	1	\$1,080.00	1	\$1,080.00
29	SPOT	08/29/2019	08/29/2019	08/29/2019	1	\$1,080.00	1	\$1,080.00
30	SPOT	08/30/2019	08/30/2019	08/30/2019	1	\$1,080.00	1	\$1,080.00
31	SPOT	08/31/2019	08/31/2019	08/31/2019	1	\$1,080.00	1	\$1,080.00

The number of image tokens:

VDInstruct: 40

Qwen2VL: 1290

LLaVA 1.5: 576

DocOwl 1.5: 1799

The number of image tokens:

VDInstruct: 698

Qwen2VL: 1312

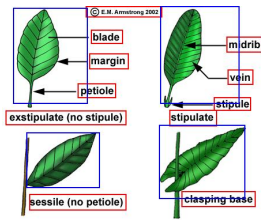
LLaVA 1.5: 576

DocOwl 1.5: 1799

Figure 5. The number of image tokens encoded by VDIINSTRUCT and its counterparts. The red and blue boxes cover the detected text and vision ROIs, respectively. Our dual vision encoder scales the number of image tokens with the detected contents, minimizing token redundancy and information loss.

Setting	Stage 1: Spatial Encoder	Stage 2: Feature Learning	Stage 3: Instruction Finetuning
Hardware	8×NVIDIA RTX A6000 (48GB)	3×NVIDIA A100-SXM (40GB)	3×NVIDIA A40 (48GB)
Batch size	16	12	48
DeepSpeed	ZeRO2	ZeRO2	ZeRO2
LoRA	-	-	rank=128, alpha=256
Epochs	10	1	1
Precision	Full (fp32)	Half (fp16)	Half (fp16)
Learning rate	1e-4	2e-5	1e-4 (projector: 2e-5)
Warmup ratio	0.1	0.03	0.03
Weight decay	0.0	0.0	0.01
Training time	1 day	7.5 days	19 hours

Table 8. Training settings for the three-stage training paradigm.



AI2D



SROIE

KJZZ
298 S Main St
Salt Lake City UT 84111

Col (G) Governor: R
280 S 400 W STE 200
SALT LAKE CITY UT 84101-1888

Contract # 4388171

Schedule Dates 05/08/20-09/11/20

Advertiser Col (G) Governor: R (133788)

Agency Scripps (5599)

Product POLITICAL CANDIDATE (11185)

Brand TV3000 POL GOVERNOR (1349360)

Salesperson HOUSESAL LAKE CITY/KUTV/KMYU/KJZZ (3005)

Sales Office KUTV/KMYU/KJZZ

Buyer Name

Phone/Fax

CPE 65/1736205

Account Types Local/Political/Candidate/Agency (30)

Billing Type Weekly/Regular

Comments Election '20

Estimate # 5691720

Estimate Date 05/08/20

Entered # 5691720

CO-OP Ad

External # 5691720

Order # 23518

Order Type Normal

Package Deal

Commission % 15.00

Commission \$108.00

Net Total \$517.00

Gross Total

Salt Lake City (KJZZ)

Line	Product	Start	End	Spots	Rate
1	HOUSESAL LAKE CITY	05/08/20	09/11/20	1	\$200.00
2	HOUSESAL LAKE CITY	05/08/20	09/11/20	1	\$200.00

Line	Product	Start	End	Spots	Rate	Commission	Net Total
1	HOUSESAL LAKE CITY	05/08/20	09/11/20	1	\$200.00	\$30.00	\$170.00
2	HOUSESAL LAKE CITY	05/08/20	09/11/20	1	\$200.00	\$30.00	\$170.00
3	HOUSESAL LAKE CITY	05/08/20	09/11/20	1	\$200.00	\$30.00	\$170.00
4	HOUSESAL LAKE CITY	05/08/20	09/11/20	1	\$200.00	\$30.00	\$170.00
5	HOUSESAL LAKE CITY	05/08/20	09/11/20	1	\$200.00	\$30.00	\$170.00
6	HOUSESAL LAKE CITY	05/08/20	09/11/20	1	\$200.00	\$30.00	\$170.00
7	HOUSESAL LAKE CITY	05/08/20	09/11/20	1	\$200.00	\$30.00	\$170.00
8	HOUSESAL LAKE CITY	05/08/20	09/11/20	1	\$200.00	\$30.00	\$170.00
9	HOUSESAL LAKE CITY	05/08/20	09/11/20	1	\$200.00	\$30.00	\$170.00
10	HOUSESAL LAKE CITY	05/08/20	09/11/20	1	\$200.00	\$30.00	\$170.00
11	HOUSESAL LAKE CITY	05/08/20	09/11/20	1	\$200.00	\$30.00	\$170.00
12	HOUSESAL LAKE CITY	05/08/20	09/11/20	1	\$200.00	\$30.00	\$170.00
13	HOUSESAL LAKE CITY	05/08/20	09/11/20	1	\$200.00	\$30.00	\$170.00
14	HOUSESAL LAKE CITY	05/08/20	09/11/20	1	\$200.00	\$30.00	\$170.00
15	HOUSESAL LAKE CITY	05/08/20	09/11/20	1	\$200.00	\$30.00	\$170.00
16	HOUSESAL LAKE CITY	05/08/20	09/11/20	1	\$200.00	\$30.00	\$170.00
17	HOUSESAL LAKE CITY	05/08/20	09/11/20	1	\$200.00	\$30.00	\$170.00
18	HOUSESAL LAKE CITY	05/08/20	09/11/20	1	\$200.00	\$30.00	\$170.00
19	HOUSESAL LAKE CITY	05/08/20	09/11/20	1	\$200.00	\$30.00	\$170.00
20	HOUSESAL LAKE CITY	05/08/20	09/11/20	1	\$200.00	\$30.00	\$170.00
21	HOUSESAL LAKE CITY	05/08/20	09/11/20	1	\$200.00	\$30.00	\$170.00
22	HOUSESAL LAKE CITY	05/08/20	09/11/20	1	\$200.00	\$30.00	\$170.00
23	HOUSESAL LAKE CITY	05/08/20	09/11/20	1	\$200.00	\$30.00	\$170.00
24	HOUSESAL LAKE CITY	05/08/20	09/11/20	1	\$200.00	\$30.00	\$170.00
25	HOUSESAL LAKE CITY	05/08/20	09/11/20	1	\$200.00	\$30.00	\$170.00
26	HOUSESAL LAKE CITY	05/08/20	09/11/20	1	\$200.00	\$30.00	\$170.00
27	HOUSESAL LAKE CITY	05/08/20	09/11/20	1	\$200.00	\$30.00	\$170.00
28	HOUSESAL LAKE CITY	05/08/20	09/11/20	1	\$200.00	\$30.00	\$170.00
29	HOUSESAL LAKE CITY	05/08/20	09/11/20	1	\$200.00	\$30.00	\$170.00
30	HOUSESAL LAKE CITY	05/08/20	09/11/20	1	\$200.00	\$30.00	\$170.00
31	HOUSESAL LAKE CITY	05/08/20	09/11/20	1	\$200.00	\$30.00	\$170.00
32	HOUSESAL LAKE CITY	05/08/20	09/11/20	1	\$200.00	\$30.00	\$170.00
33	HOUSESAL LAKE CITY	05/08/20	09/11/20	1	\$200.00	\$30.00	\$170.00
34	HOUSESAL LAKE CITY	05/08/20	09/11/20	1	\$200.00	\$30.00	\$170.00
35	HOUSESAL LAKE CITY	05/08/20	09/11/20	1	\$200.00	\$30.00	\$170.00
36	HOUSESAL LAKE CITY	05/08/20	09/11/20	1	\$200.00	\$30.00	\$170.00
37	HOUSESAL LAKE CITY	05/08/20	09/11/20	1	\$200.00	\$30.00	\$170.00
38	HOUSESAL LAKE CITY	05/08/20	09/11/20	1	\$200.00	\$30.00	\$170.00
39	HOUSESAL LAKE CITY	05/08/20	09/11/20	1	\$200.00	\$30.00	\$170.00
40	HOUSESAL LAKE CITY	05/08/20	09/11/20	1	\$200.00	\$30.00	\$170.00
41	HOUSESAL LAKE CITY	05/08/20	09/11/20	1	\$200.00	\$30.00	\$170.00
42	HOUSESAL LAKE CITY	05/08/20	09/11/20	1	\$200.00	\$30.00	\$170.00
43	HOUSESAL LAKE CITY	05/08/20	09/11/20	1	\$200.00	\$30.00	\$170.00
44	HOUSESAL LAKE CITY	05/08/20	09/11/20	1	\$200.00	\$30.00	\$170.00
45	HOUSESAL LAKE CITY	05/08/20	09/11/20	1	\$200.00	\$30.00	\$170.00
46	HOUSESAL LAKE CITY	05/08/20	09/11/20	1	\$200.00	\$30.00	\$170.00
47	HOUSESAL LAKE CITY	05/08/20	09/11/20	1	\$200.00	\$30.00	\$170.00
48	HOUSESAL LAKE CITY	05/08/20	09/11/20	1	\$200.00	\$30.00	\$170.00
49	HOUSESAL LAKE CITY	05/08/20	09/11/20	1	\$200.00	\$30.00	\$170.00
50	HOUSESAL LAKE CITY	05/08/20	09/11/20	1	\$200.00	\$30.00	\$170.00
51	HOUSESAL LAKE CITY	05/08/20	09/11/20	1	\$200.00	\$30.00	\$170.00
52	HOUSESAL LAKE CITY	05/08/20	09/11/20	1	\$200.00	\$30.00	\$170.00
53	HOUSESAL LAKE CITY	05/08/20	09/11/20	1	\$200.00	\$30.00	\$170.00
54	HOUSESAL LAKE CITY	05/08/20	09/11/20	1	\$200.00	\$30.00	\$170.00
55	HOUSESAL LAKE CITY	05/08/20	09/11/20	1	\$200.00	\$30.00	\$170.00
56	HOUSESAL LAKE CITY	05/08/20	09/11/20	1	\$200.00	\$30.00	\$170.00
57	HOUSESAL LAKE CITY	05/08/20	09/11/20	1	\$200.00	\$30.00	\$170.00
58	HOUSESAL LAKE CITY	05/08/20	09/11/20	1	\$200.00	\$30.00	\$170.00
59	HOUSESAL LAKE CITY	05/08/20	09/11/20	1	\$200.00	\$30.00	\$170.00
60	HOUSESAL LAKE CITY	05/08/20	09/11/20	1	\$200.00	\$30.00	\$170.00
61	HOUSESAL LAKE CITY	05/08/20	09/11/20	1	\$200.00	\$30.00	\$170.00
62	HOUSESAL LAKE CITY	05/08/20	09/11/20	1	\$200.00	\$30.00	\$170.00
63	HOUSESAL LAKE CITY	05/08/20	09/11/20	1	\$200.00	\$30.00	\$170.00
64	HOUSESAL LAKE CITY	05/08/20	09/11/20	1	\$200.00	\$30.00	\$170.00
65	HOUSESAL LAKE CITY	05/08/20	09/11/20	1	\$200.00	\$30.00	\$170.00
66	HOUSESAL LAKE CITY	05/08/20	09/11/20	1	\$200.00	\$30.00	\$170.00
67	HOUSESAL LAKE CITY	05/08/20	09/11/20	1	\$200.00	\$30.00	\$170.00
68	HOUSESAL LAKE CITY	05/08/20	09/11/20	1	\$200.00	\$30.00	\$170.00
69	HOUSESAL LAKE CITY	05/08/20	09/11/20	1	\$200.00	\$30.00	\$170.00
70	HOUSESAL LAKE CITY	05/08/20	09/11/20	1	\$200.00	\$30.00	\$170.00
71	HOUSESAL LAKE CITY	05/08/20	09/11/20	1	\$200.00	\$30.00	\$170.00
72	HOUSESAL LAKE CITY	05/08/20	09/11/20	1	\$200.00	\$30.00	\$170.00
73	HOUSESAL LAKE CITY	05/08/20	09/11/20	1	\$200.00	\$30.00	\$170.00
74	HOUSESAL LAKE CITY	05/08/20	09/11/20	1	\$200.00	\$30.00	\$170.00
75	HOUSESAL LAKE CITY	05/08/20	09/11/20	1	\$200.00	\$30.00	\$170.00
76	HOUSESAL LAKE CITY	05/08/20	09/11/20	1	\$200.00	\$30.00	\$170.00
77	HOUSESAL LAKE CITY	05/08/20	09/11/20	1	\$200.00	\$30.00	\$170.00
78	HOUSESAL LAKE CITY	05/08/20	09/11/20	1	\$200.00	\$30.00	\$170.00
79	HOUSESAL LAKE CITY	05/08/20	09/11/20	1	\$200.00	\$30.00	\$170.00
80	HOUSESAL LAKE CITY	05/08/20	09/11/20	1	\$200.00	\$30.00	\$170.00
81	HOUSESAL LAKE CITY	05/08/20	09/11/20	1	\$200.00	\$30.00	\$170.00
82	HOUSESAL LAKE CITY	05/08/20	09/11/20	1	\$200.00	\$30.00	\$170.00
83	HOUSESAL LAKE CITY	05/08/20	09/11/20	1	\$200.00	\$30.00	\$170.00
84	HOUSESAL LAKE CITY	05/08/20	09/11/20	1	\$200.00	\$30.00	\$170.00
85	HOUSESAL LAKE CITY	05/08/20	09/11/20	1	\$200.00	\$30.00	\$170.00
86	HOUSESAL LAKE CITY	05/08/20	09/11/20	1	\$200.00	\$30.00	\$170.00
87	HOUSESAL LAKE CITY	05/08/20	09/11/20	1	\$200.00	\$30.00	\$170.00
88	HOUSESAL LAKE CITY	05/08/20	09/11/20	1	\$200.00	\$30.00	\$170.00
89	HOUSESAL LAKE CITY	05/08/20	09/11/20	1	\$200.00	\$30.00	\$170.00
90	HOUSESAL LAKE CITY	05/08/20	09/11/20	1	\$200.00	\$30.00	\$170.00
91	HOUSESAL LAKE CITY	05/08/20	09/11/20	1	\$200.00	\$30.00	\$170.00
92	HOUSESAL LAKE CITY	05/08/20	09/11/20	1	\$200.00	\$30.00	\$170.00
93	HOUSESAL LAKE CITY	05/08/20	09/11/20	1	\$200.00	\$30.00	\$170.00
94	HOUSESAL LAKE CITY	05/08/20	09/11/20	1	\$200.00	\$30.00	\$170.00
95	HOUSESAL LAKE CITY	05/08/20	09/11/20	1	\$200.00	\$30.00	\$170.00
96	HOUSESAL LAKE CITY	05/08/20	09/11/20	1	\$200.00	\$30.00	\$170.00
97	HOUSESAL LAKE CITY	05/08/20	09/11/20	1	\$200.00	\$30.00	\$170.00
98	HOUSESAL LAKE CITY	05/08/20	09/11/20	1	\$200.00	\$30.00	\$170.00
99	HOUSESAL LAKE CITY	05/08/20	09/11/20	1	\$200.00	\$30.00	\$170.00
100	HOUSESAL LAKE CITY	05/08/20	09/11/20	1	\$200.00	\$30.00	\$170.00

Deepform

Figure 6. Qualitative results on multimodal RoI detection. The red boxes indicate the text regions, while the blue boxes indicate the vision regions. In general, the RoI detector module performs well in various document types with different resolutions.